LAMINAR COMPOSITE WING SURFACE WAVINESS - TWO COUNTERACTING EFFECTS AND A COMBINED ASSESSMENT BY TWO METHODS

L. Heinrich, Deutsches Zentrum für Luft- und Raumfahrt, Institut für Faserverbundleichtbau und Adaptronik, Lilienthalplatz 7, Braunschweig, Deutschland

M. Kruse, Deutsches Zentrum für Luft- und Raumfahrt, Institut für Aerodynamik und Strömungstechnik, Lilienthalplatz 7, Braunschweig, Deutschland

Summary

Based on a fully designed wing box section of a generic transport aircraft, two effects are investigated leading to surface waviness, namely process induced deformations (PID) and load induced deformations (LID). A DLR in-house waviness handling tool for the analysis and superposition of multiple waviness effects is introduced and applied. It is shown, that the results differ widely whether or not the effects are evaluated together. Finally, the remaining waviness is aerodynamically analysed using established methods.

1. INTRODUCTION

For the motivation, some general numbers are inevitable: According to the Fifth Assessment Report of the Intergovernmental Panel on Climate Change (IPCC), human made CO_2-equal emissions should be reduced by at least 41% in 2050 compared to 2010 [1]. In the Aeronautical Sector, accounting for ~2% of human made CO_2 emissions, the Advisory Council for Aviation Research and Innovation in Europe (ACARE) has stated amongst its goals to have technologies and procedures available by 2050 that allow a 75% reduction in CO2 emissions per passenger kilometer (compared to 2000, [2]). This goal is roughly broken down by time steps and aircraft systems, whereby 30% reducibility is to come from increased structure efficiency by 2035. Achieving these ambitious goals necessitates the introduction of several new technologies in the next generation transport aircraft like the Airbus A30X, currently targeted for the 2030s [3].

Rossow concluded, that all the 'low-hanging fruits' in terms of further drag reduction have already been picked [4]. Common agreement exists, that the biggest remaining fruit in terms of drag reduction is Laminar Flow Control (LFC) with a potential of 7-16% depending on the use case ([5]-[7]). There are two major technology streams in LFC, namely natural laminar flow (NLF) by shaping and hybrid laminar flow control (HLFC) including active means. Both technologies have their raison d'être, but the focus here is on NLF.

Structural designers might have a vague or no understanding of laminar flow, so a brief idea is given for illustration purposes: Osborne Reynolds showed in 1883 that when a body and a surrounding fluid move relative to each other, the fluid particles in the vicinity of the body are properly ordered in layers one on top of the other, where layers do not intermix [8]. This state is called laminar. As the body moves further along, the particle movement becomes chaotic at some point, referred to as turbulent. The corresponding region close to the outer surface, where maintenance of the laminar state is striven for, is called the boundary layer.

The history of LFC is almost as long as the aeronautical one. Today, most of the phenomena associated with Laminar Flow Control are reasonably well understood and many demanding requirements to maintain the flow laminar on a lifting surface have been found. These can be summarized by:

- Configurational aspects (sweep angles, pressure gradients, nose radii, wing-belly-junction, high-lift compatibility)
- Surface quality (waviness, steps, gaps, rivet heads, roughness)
- Operational aspects (insects, dirt, de-/anti-icing, maintainability, interchangeability, free stream turbulence, noise, vibration)

The focus herein is on surface quality, and in particular on waviness. Investigations about waviness on laminar wings date back to the 1940s, when serious attempts to obtain laminar flow on aircraft lifting surfaces started ([9]-[11]). The question arose whether surface deviations could trigger premature transition (from laminar to turbulent) and how such dependencies could be quantified. Investigations up to the 1960s concluded, that production technology of that time might be incompatible with laminar/waviness requirements. Significant fractions of laminar flow had only been obtained after extensive treatment of the corresponding wing surfaces (e.g. [10], [12]).

Later in the 1970s [13] and 1980s [14], flight tests on existing wing surfaces of some small to commuter type airplanes showed good portions of laminar flow without special treatment (except for two positions in the latter case). The authors concluded, that "[…] NLF may be practical on modern production surfaces (with little sweep) for transition Reynolds numbers greater than 11×10^6. The absolute upper limit remains to be determined." While these tests clearly reflected that production technology

had developed significantly, considerable uncertainties remained. So flight tests continued on numerous airplanes in the US as well as in Europe (e.g. F-111, F-14A, VFW 614, Falcon 50/900, Dornier 228, Fokker 100, Airbus A320, ([15]-[17]). All of these recent tests (and many previous ones) had artificial gloves on their wings and hence do not provide realistic data for waviness measurement and evaluation. Still the tests delivered valuable data for this purpose, because they enhanced the empirical correlation used for numerical methods of transition prediction.

An overview of LFC (including manufacturing tolerances) is given by Joslin ([18], [19]). It includes references to some analytical evaluation criteria for manufacturing deviations. These criteria (e.g. by Fage and Carmichael) are directly applicable to a given waviness, but have their limitations and are only based on older flight tests.

All the defined requirements for a laminar wing, given above, are the result of numerous investigations, theoretically as well as in many experiments. Based thereon, the aerodynamic design of an NLF wing today is relatively robust. Regarding the structural requirements for surface quality and in particular surface waviness, the magnitudes and qualitative distributions were either generically assumed or based on measurements on existing structures. The existing structures, that are representative for the intended use case, were all structures, custom-made for the specific test and non-loadbearing. Even these structures partially required rework to fulfil the extremely high surface quality required [5]. No investigation is known to the authors that was representative regarding waviness on an airliners laminar composite wing at production scale.

The focus of the investigation is put on the wing box. As indicated above, NLF can only be maintained in regions of continuously decreasing pressure. The maximum laminar extent is roughly 60-65% of the profile chord, where pressure recovery is inevitable. This matches well with the typical position of the rear spar. Also, the leading edge waviness is not examined for reasons described below.

From the aerodynamic perspective, maintaining a laminar boundary over a wide extend of a transport aircraft wing surface seems to be achievable. Today, the main problems in bringing the technology into usage are lying in the structural design, manufacturing and assembly. Especially the demand for surface quality is challenging, as any excrescence, gap, step or surface waviness immediately deteriorates the stability of the laminar boundary layer. Consequently, such surface imperfections must be minimized in order to enable laminar technology.

In this context, the present paper addresses stringer induced surface waviness. For an integrally stiffened wing-box cover, designed for a generic medium range transport aircraft with 20° leading edge sweep angle and a Mach number Ma=0.75, two effects are studied leading to such waviness. The expected remaining waviness in flight is estimated and evaluated using empirical waviness allowables. Finally, the effects on boundary layer stability and transition location are covered.

2. INTEGRALLY STIFFENED WING BOX UPPER COVER AS A PREREQUISITE FOR LAMINAR FLOW

Looking at the manufacturing and assembly concept of a wing in general, all differentially manufactured parts (e.g. stiffeners, rib caps and spar caps) need to be connected to the skin to form the wing box. In the past, rivet connections have been widely applied. For a laminar wing, this type of connection appears very unpractical. Either turbulent wedges would cover large fractions of the surface or putty would have to cover every rivet head. Besides significant efforts for the application of the putty, this raises questions about durability and maintenance aspects. As an alternative, parts could be bonded. Bonding technology has drastically developed during the past decades, but still requires design features preventing large disbonds (usually additional rivets) as long as non-destructive inspection technology proves to be reliable at production scale [20].

In order to completely avoid local disturbances by discrete connecting elements, a fully integral wing upper cover has been designed and manufactured in the German Government funded projects LaWiPro ([21]-[23]) and MOVE.ON – LaWOp (FIG. 1). The wing geometry is based on the NLF13 research configuration, commonly used by all partners [23]. The entire wing cover including longitudinal stiffeners and caps for the attachment of ribs and spars is manufactured in one part. By this means, connecting elements on the outer surface are completely avoided. As a consequence, an innovative manufacturing concept including hollow cores had to be developed ([21], [22], [24]).

The overall concept includes Krüger flaps for high-lift and insect shielding. A separate nose is designed to fulfil the requirements about maintainability and interchangeability. It features and innovative assembly concept that precisely and quickly attaches to the overhang of the upper skin (left side on FIG. 1).

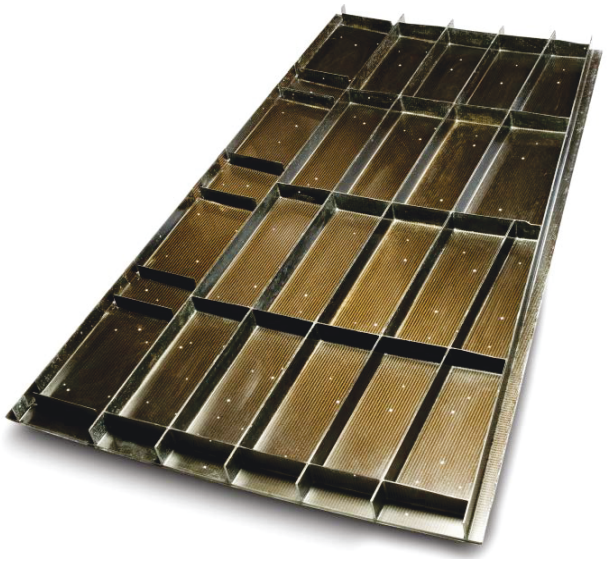

FIG. 1. Inside view on the manufactured upper cover with integral stiffeners and caps

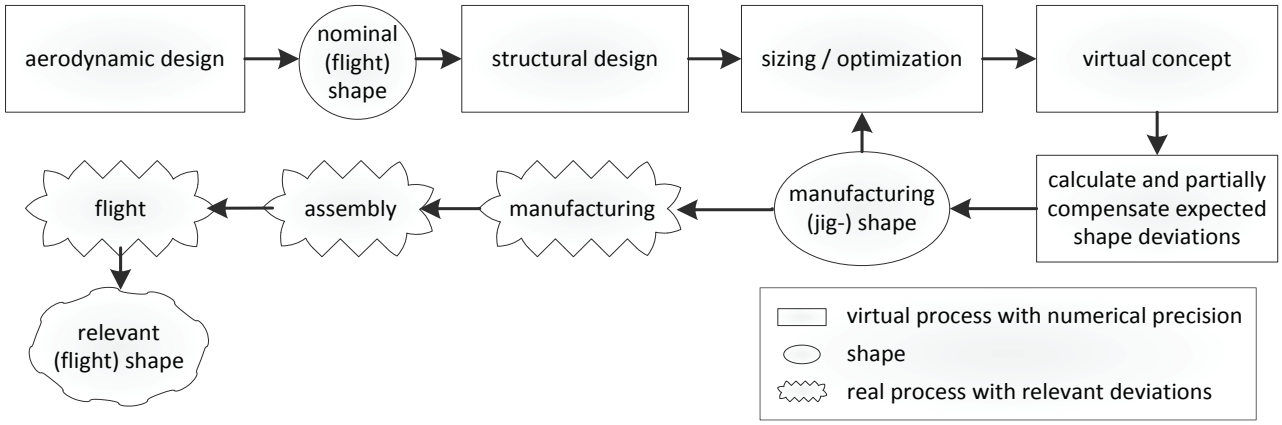

FIG. 2. Aerodynamic and structural steps in the genesis of an aircraft with emphasis on shape deviations

3. DEFORMATION EFFECTS

Lightweight design is mandatory for the operation of large transport airplanes to be profitable. In the 1910s, a new type of airplane load bearing structure emerged [25]. In contrast to other airplanes of that time, these structures consisted of a stiff but relatively thin skin, usually made out of several plies of wood. This shell type structure, later known as semi-monocoque, was reinforced in one or two directions by stiffeners, leading to an excellent ratio of weight and loading capacity. Nowadays, all major airliners utilize load bearing structures of semi-monocoque type in their wings and fuselages. Sandwich as an alternative has not evolved for several reasons ([26], [27]).

Structures of semi-monocoque type inherently have a distinct inhomogeneous distribution of the bending stiffness. This inhomogeneity clearly increases the material utilization on the one hand. On the other hand, several additional aspects have to be regarded, e.g. additional stability modes and the skin-stiffener interface. Concerning the requirements of a laminar wing, it is quite obvious, that the aerodynamic loads, acting across such a discretely stiffened structure, induce some waviness. This effect will be called load induced deformations (LID) in the following.

The aforementioned advantages of a fully integral wing cover for NLF are accompanied by some challenges. For the process of composite manufacturing, it is well known that there exists a certain correlation between shape complexity of an integral part and its manufacturing induced deviations. The parameters and phenomena associated with this correlation were subject of many investigations, e.g. [28]-[31]. In relation to waviness of a stiffened panel, the effects of spring-in and forced interaction are dominant [32].

In the context herein, shape deviations during the manufacturing process are termed process induced deviations (PID). For the prediction of PID, an efficient method was developed and validated by Kappel [31]. In contrast to classical simulation approaches for the manufacturing process, it features small modelling efforts based on shell elements while requiring only engineering-like parameters, typically gained from laboratory-scale L-profile specimens.

After the manufacturing of a wings parts (with PID), all parts have to be assembled. The wing assembly is a third step with inherent shape deviations. The assembly of real parts is a highly complex process in itself that requires its own conceptual approach, in particular for a laminar wing. This is out of the scope here.

All three processes (manufacturing, assembly and flight) with inherent shape deviations are depicted in FIG. 2, together with the disciplinary design steps which initially can affect these deviations. The purpose of this is to illustrate the high demands that the structural design of a laminar wing poses. Today, designing and dimensioning a CFRP wing including pre-computation and consideration of expected global wing deformations during cruise flight has been mastered for the first transport aircraft. In order to design a laminar wing, one ought to precisely anticipate and account for local shape deviations from all three processes mentioned.

4. PID AND LID – NUMERICAL QUANTIFICATION

In the numerical quantifications herein, the assembly is incorporated by applying appropriate boundary conditions. Interface regions to other parts are rigidly held in place, corresponding to a perfect assembly. Still there are two effects contributing to the relevant shape of the outer skin during flight (and they are expected to prevail). This raises questions:

- How do they combine?
- Can they be evaluated individually?
- Are they within the required limits?

As a first step, both waviness effects are numerically quantified. Baseline is the detailed design model, featuring all relevant aspects including ply stacking sequences. There are several flight mission segments where the boundary layer could be kept laminar. The most promising one (in terms of potential and attainability) is the cruise flight. Hence, the focus herein is put on this segment only. Furthermore, both effects are quantified individually. Especially for the LID, it is assumed that they are independent of the previously occurring PID and also of the global wing bending.

A complete structural design of a wing nose, representative for a laminar composite wing, was not available for this study; so waviness was analysed on the wing upper cover only. Due to the high curvature and bird strike requirements, waviness on the wing nose is expected to be less critical than for the wing box.

Kappel recently developed different modeling approaches [33] for the method of PID prediction [30]. By the time of this study, the approach that was available and validated included modeling of radii between stiffeners and the outer skin. As the detailed design model did not include these radii, a second model was built for estimating PID.

Looking at the z-displacement contours of PID (FIG. 3) and LID (FIG. 4), several peculiarities are conspicuous (with z being almost normal to the outer surface). Most obvious are the differences in the magnitude and in the characteristic. Both plots have been created using the same absolute range of values, but the colour spectrum of the PID is reverted. Thus, colours and values of both plots directly correlate, but with inverted directions. The PIDs magnitude exceeds the LIDs one all across the range of evaluation, but they are in the same order.

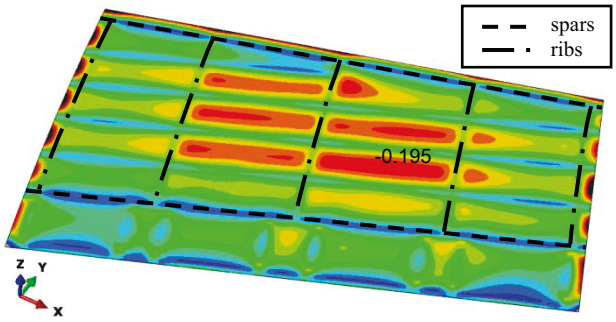

FIG. 3. Expected process induced deviations (PID, z) after manufacturing

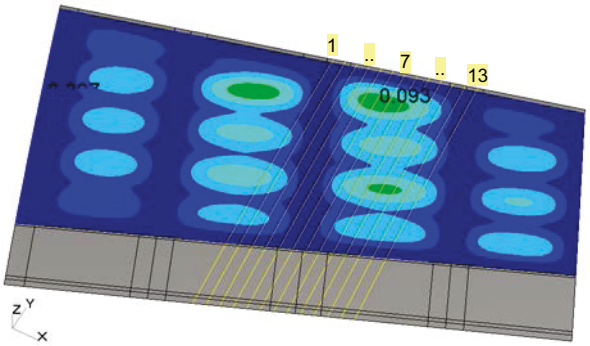

FIG. 4. Expected load induced deformations (LID, z) during cruise flight

The characteristic of the PID is more plateau-like. Adjacent to the stringers, the PID is rapidly rising towards the middle of a skin field, whereas the slope of the LID is clearly lower. This principal difference can be attributed to the dissimilar ranges of the effects' causes. The aerodynamic loads are distributed continuously across the outer skin, whereas the spring-in effect as the main cause for waviness from PID is acting localized at the stringer-skin- and cap-skin-interfaces.

As expected, the two effects are acting in opposite directions. Manufacturing deviations deflect the outer skin towards the inside of the wing, whereas the pressure difference deflects the skin towards the outside. Furthermore, the magnitudes of both effects at the rib segments in the middle are higher than at the rib segments located at the parts boundaries. This can be attributed to the higher rib distance at these stations.

5. WAVINESS ANALYSIS IN CROSS-SECTIONS

The assessment of the waviness must be done in cross-sections because all methods available for the aerodynamic evaluation are based on two-dimensional treatment. Cross sections are commonly extracted in flight direction, which in steady flight corresponds to the y-z-plane. As the wing is swept and the ribs are defined normal to the leading edge (FIG. 4), the waviness characteristic in flight direction depends on the spanwise position. In order to cover representative waviness characteristics and potentially identify trends, 13 equidistant cross-sections along the rib segment with the biggest shape deviations are taken (the intersection curves are shown in FIG. 4). For descriptive purposes, they have been enumerated from 1 (at x=13.16m) to 13 (at x=13.76m).

The workflows in relation to waviness assessment can be manifold. In this paper, two waviness effects, based on numerical finite element models, are merged. But there may be other sources of waviness (e.g. the wing assembly) or other data sources (e.g. measurements together with CAD data as reference). Some waviness effects may require post-processing before being ready for merging. For subsequent assessment, waviness might have to be transferred to some substitute profile. In order to enable all these workflows, the tool PyWaves has been written in the python™ programming language. It enables reading data in several formats, automatic pre-alignment into a common coordinate system, established functionalities for the analysis, interpolation and editing of geometrical data in cross-sections as well as features for waviness assessment. An overview of the functionalities, sorted by general steps of data handling, is depicted in FIG. 5.

A detailed description of PyWaves is out of the scope here. It is very efficient, which enables analysis and processing on-the-fly. This is further supported by an intuitive interface with detailed reporting of work steps, instant creation of graphs and saving of relevant data for later usage. An excerpt can be seen in FIG. 6 in the following section.

In order to enable diverse workflows, three levels of abstraction have been implemented for the structuring of functionalities and data handling (TAB 1).

Class	Scope of data and functions
Cut	Individual cross-section
Representation	An individual waviness effect
PointCloud	A single point cloud

TAB 1. Abstraction levels for the programming approach

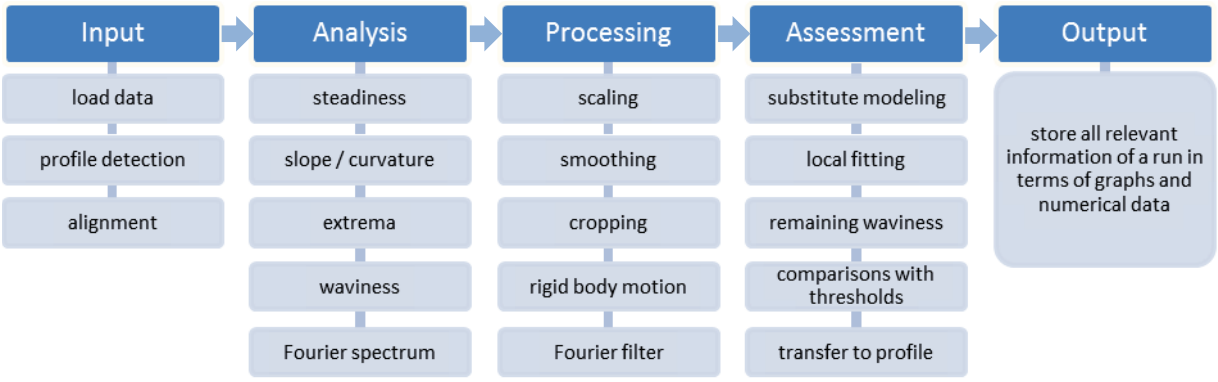

FIG. 5. Overview of PyWaves functionalities

6. DIRECT EVALUATION USING BOUNDARY VALUES

Several attempts were made to establish criteria for permissible waviness. For a reliable structural design of a laminar wing, this is of utmost importance. Older criteria (e.g. [34], [35]) are publicly available and have their known limitations [36]. For a structural designer, their important benefit is the direct applicability to a given waviness. After the relaunch of laminar research in the early 80s, the focus of aerodynamic investigations turned towards the numerical transition prediction (like in the next section). These predictions were (and still are) empirically based, but they include the progressions in the aerodynamic understanding of the transition mechanisms (namely Tollmien-Schlichting- and crossflow- instabilities) and also more recent flight tests. Although there still is a huge amount of scatter in the empirical correlations, these prediction methods are assumed to be more precise and more generally applicable. But in order to design a laminar wing from the structural viewpoint, they are barely helpful. No publicly available waviness criteria is known that is directly applicable while including the abovementioned progressions. The most promising approach seems to be an empirical correlation equation, based on ΔN-values [36], which (to the authors' opinions) still requires some advancement for being generally applicable.

In this section, the publicly available Carmichael criterion (initially published in 1959) is used. Although developed for wings with suction and having other limitations, it is still adequate for the purpose herein, which is to qualitatively illustrate the differences between individual and combined assessment. The two waviness effects regarded are contributing to the relevant flight shape (FIG. 2). If one wanted to evaluate an effect individually while knowing about this common contribution, the only feasible way would be to halve the allowable amplitudes, because in the worst case, both effects would point in the same direction and have the same amplitude.

The Carmichael criterion for a single wave is given as (from [18]):

$$(1) \quad \frac{a}{\lambda} = \left(\frac{59000\, c\, \cos^2 \Lambda}{\lambda\, Re_c^{3/2}} \right)^{1/2}$$

with the amplitude a, the full sinuous wavelength λ, the chord length c, the leading edge sweep angle Λ and Re_c, corresponding to the chord Reynolds number. For the current case (TAB 2) and a factor of one third accounting for multiple waves, this yields:

$$(2) \quad a = 0.014203\, \lambda^{1/2}$$

In FIG. 6, waviness from PID and LID is exemplarily shown together with their remaining waviness for cut no. 6 (refer to FIG. 4). Minor smoothing (especially at the borders) was required, primarily to obtain wavy profiles of good quality for subsequent numerical assessment. Furthermore the evaluation by Carmichael criterion can be seen for each half-wave in terms of a RF-label. The allowable waviness for individual evaluation of the effects has been halved as described above. The RF-values are the factors, by whom the wave height would have to be scaled in order to just be acceptable.

Cut no. 6 has been selected, because it illustrates well the different characteristics in the individual effects and in their interaction. At the front spar (left side of the figure), this cut is close to a rib, which acts like a clamping. With two holding elements nearby (rib and spar), the continuous aero-loads are too small to lead to distinct deformations. For the PID, there are also two radii imposing noticeable deviations. So the remaining waviness close to the front spar is dominated by the PID. In the rear part of the cross section, especially in the last skin field before the rear spar, both effects are nearly equal in size, leading to a change in the characteristic of the remaining waviness.

Regarding the waviness evaluation, and in particular comparing individual versus combined assessment, the RF-values differ quite arbitrarily. The remaining waviness' RF-values are all within the required limits; the individual assessment can over- or underestimate the criticality of the remaining waviness. PID was even evaluated to be unacceptable in two cases. Hence it can be followed, that waviness of multiple effects requires a combined assessment in order to yield reasonable results.

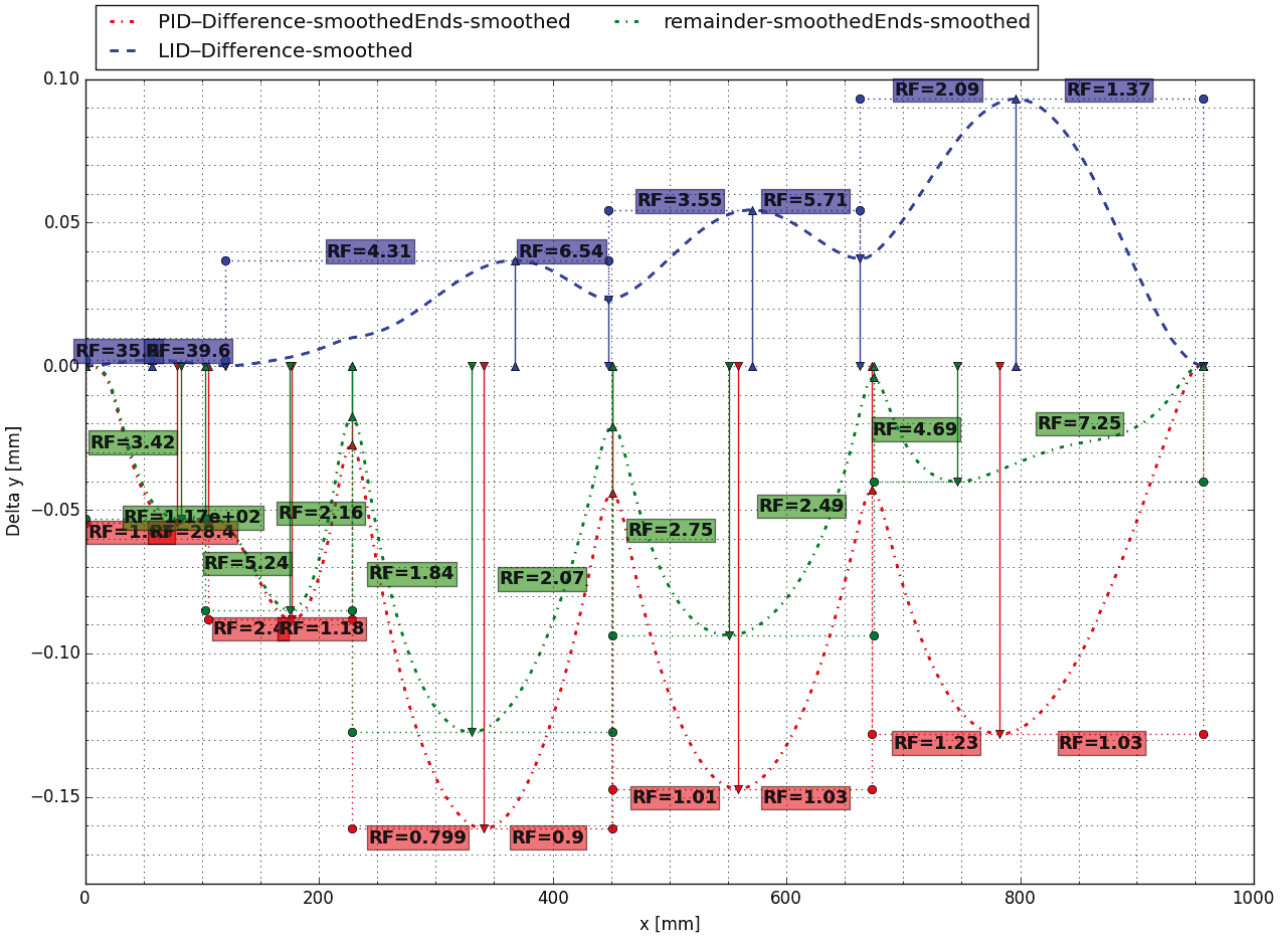

FIG. 6. Cut no. 6 with typical distribution of waviness effects, their remainder and applied Carmichael criterion

7. AERODYNAMIC ANALYSIS OF WAVY WING SECTIONS

Aerodynamic studies are conducted to assess the potential impact of stringer-induced waviness on the boundary layer stability of the Airbus NLF13 research configuration (FIG. 7). The outer wing section, for which the integral stringer-stiffened upper cover was designed, is regarded under cruise flight conditions.

7.1. Design of an aerodynamic substitute section

Since the effort for a full 3D stability analysis of the boundary layer flow past the three-dimensional wavy surface of the wing is highly demanding and impractical within the limits of this study, a simplified aerodynamic model is considered. Using the inverse design method of Bartelheimer/Takanashi [37], we derive a clean, non-wavy infinite swept wing model, representing the aerodynamic characteristics of the reference outer wing section at cruise flight. TAB 2 summarizes figures derived from the 3D wing section and transferred to the substitute infinite swept wing by inverse design. FIG. 8 gives a comparison of c_p-distributions for the 3D wing section and the designed infinite swept wing model. As shown, a close match is obtained, intentionally avoiding the adverse leading edge c_p peak from the 3D solution in 2.5D design.

spanwise reference section	y_{ref} =	13.46	m
local chord length	c_{ref} =	2.573	m
chord Reynolds number	Re_c =	17.6E6	-
local lift coefficient	$c_l(y_{ref})$ =	0.62	-
freestream Mach number	Ma_∞ =	0.75	-
LE sweep angle (3D) / sweep angle (2.5D)	φ =	20	°

TAB 2. Key figures of NLF13 outer reference section used for inverse design

7.2. Application of surface waviness to the substitute section

The creation of wavy airfoil sections is done by superposition of normalized coordinates of waviness data to the substitute 2.5D airfoil section. Waviness data for the designed upper wing box cover (FIG. 1) is provided in 13 spanwise slices. As shown in FIG. 4, a fair coverage of spanwise wave shape variation is obtained. Distinction is made between process-induced waviness (PID) and (air-)load-induced waviness (LID), in order to allow for individual or combined analysis. A spline-based interpolation routine is employed for superposition of coordinates, enabling for a flexible and accurate way to

create wavy airfoil sections. Output for subsequent CFD mesh generation is provided in iges-format.

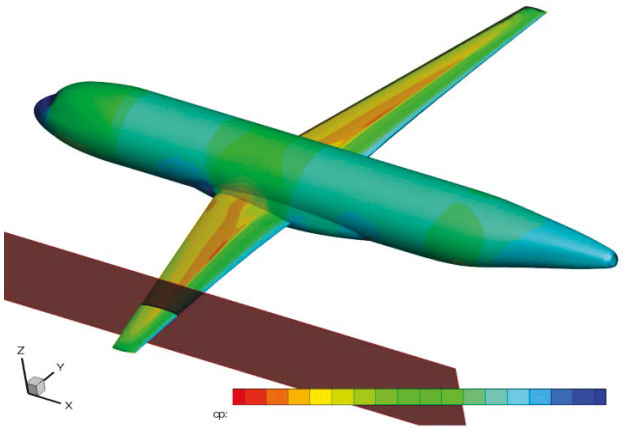

FIG. 7. Surface pressure coefficient of the Airbus NLF13 wing-body configuration and location of the reference outer wing section.

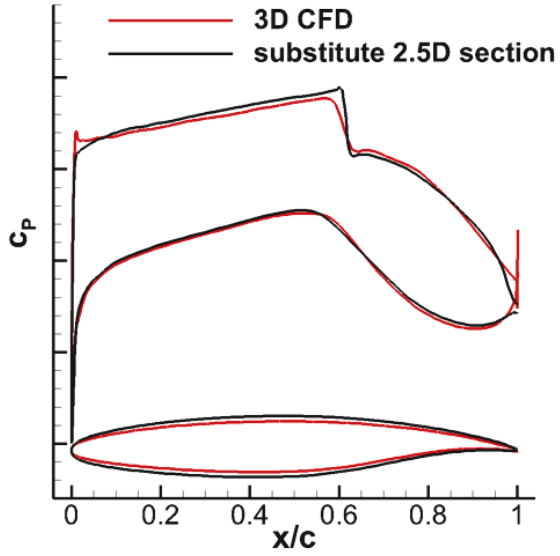

FIG. 8. Comparison of pressure coefficients from 3D CFD solution at reference section and designed infinite swept wing model.

7.3. CFD mesh generation, numerical flow simulation and stability analysis

To reveal the impact of small-scale surface waviness on the flow field and the boundary layer stability in particular, a high spatial resolution is mandatory. For this study, mixed-element hybrid grids with a structured near surface resolution of 1000x156 cells are created. Commercial mesh generation software *GRIDGEN* V15 is used. To ensure constant mesh quality, the whole process of waviness superposition, geometry generation and script-based mesh generation runs automated. Accuracy of geometry representation is checked to be better than 1E-8m, which is three orders smaller than typical wave amplitude.

DLR's RANS flow solver *TAU* [38] is employed for the calculation of steady-state flow solutions past wavy infinite swept wing sections. Periodic boundary conditions are used to establish infinite swept wing conditions.

A second-order finite-differences scheme with low-Mach number preconditioning is utilized to obtain accurate solutions, especially important w.r.t. the highly resolved boundary layer. For the main objective to analyze waviness impact on laminar boundary layer stability, all simulations were run with prescribed transition locations at x/c=0.602 on the upper surface and x/c=0.06 on the lower surface at first. Movement of transition location is treated in a second step. It is to mention, that all calculations were carried out for the same reference chord Reynolds number of Re_c=17.6E6 although the chord length of the 13 slices used for waviness extraction varies. This approach is chosen, in order to make results for different wave shapes directly comparable.

Stability analysis of the laminar boundary layer flow is conducted by compressible, local linear stability solver *lilo* [39]. As mentioned previously, input data is directly derived from the RANS flow solution. A fixed frequency/fixed wavelength 2-N-Factor method [40] is employed, where streamwise Tollmien-Schlichting instability (TS) and cross-flow instability (CF) are treated independently. Cross-flow analysis is limited to stationary waves here, since these are usually dominant under low-turbulence freestream conditions. To predict movement of the transition location due to waviness, e^N-Method is employed. The standard N_{TS}-N_{CF} limiting curve of *lilo* is used.

7.4. Summary of results and discussion

At first, the characteristics of the non-wavy substitute model are studied. FIG. 9 shows Mach number isolines of the flow field. Along the upper surface NLF branch, a smooth, continuous acceleration takes place. The supersonic region ends with a moderate normal shock at x/c=0.6. Up to this point, the growth of Tollmien-Schlichting and cross flow instabilities is subcritical and the boundary layer remains laminar. From FIG. 10 we see that TS-modes are the dominant type of instability here. No separation is observed downstream of the shock. The flow field past the lower surface remains subsonic. No effort of stability calculation is made for the lower side, where transition is prescribed at x/c=0.06. Summarizing, the non-wavy infinite swept wing section represents a classic transonic NLF design.

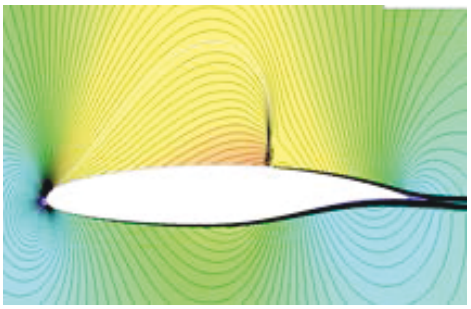

FIG. 9. Mach contour isolines of the clean, non-wavy infinite swept wing section at M=0.75, c_L=0.62, Re=17.6E6

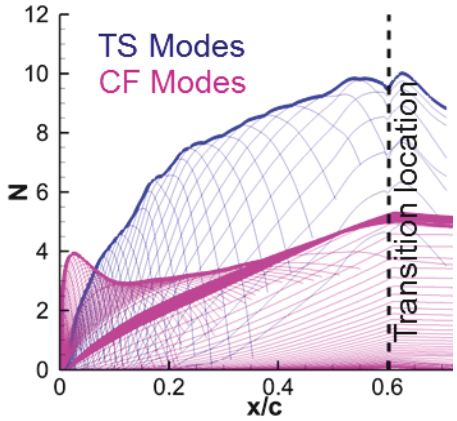

FIG. 10. N-Factor development over normalized chord length, upper side, non-wavy section.

The impact of surface waviness on boundary layer stability has been analyzed for the 13 waviness distributions extracted from the upper wing box cover. In this section, results obtained for waviness of slice no. 6 (see FIG. 6) will be discussed exemplarily. In FIG. 11, a comparison of the influence of PID-waviness, LID-waviness and combined PID/LID waviness w.r.t. envelopes for TS- and CF-instabilities is given.

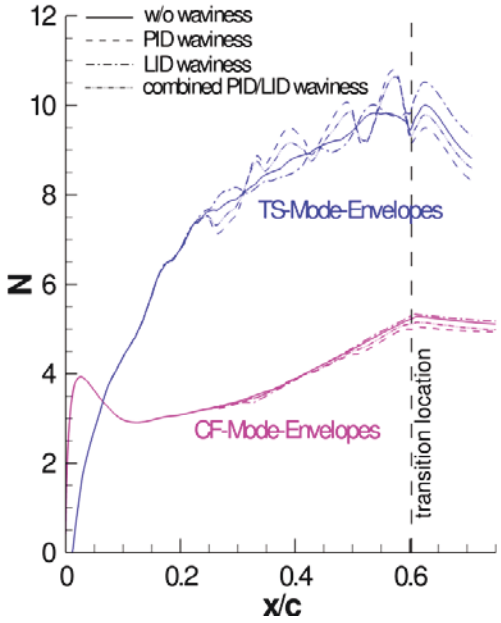

FIG. 11. Envelopes of N-Factors for TS and CF instabilities. Comparison of non-wavy reference vs. section with PID-, LID and combined waviness

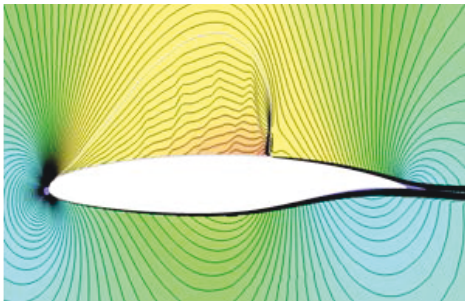

FIG. 12. Mach contour & isolines, infinite swept wing section with combined PID/LID waviness.

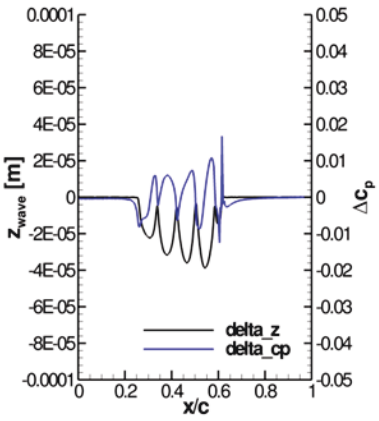

FIG. 13. Magnitude of combined PID/LID waviness over normalized chord length and resulting difference in c_p distribution w.r.t. non-wavy section.

Obviously, TS-instability reacts very sensitive to surface waviness, whereas the cross-flow N-factor is merely affected by the waves oriented perpendicular to streamwise flow direction. Each stringer induced wave causes an oscillation of the N-factor around its reference value obtained for the non-wavy section. It is noteworthy, that no clear sign of disturbance amplitude accumulation past the waves is given by the results obtained from linear stability theory (LST). Studies of Wie and Malik [36] relate this behavior to the neglect of non-local effects in LST. Thus, LST usually will underpredict the destabilizing effect of waviness. As shown in FIG. 11, the amplitude of TS-N-factors is similar at the transition location, with or without waviness. Predicted movement of transition location will be mostly due to wave-induced overshoots of the local N-factor beyond critical limits.

Comparing the impact of PID and LID waviness for this particular case, the higher amplitude of PID waviness causes higher disturbances of the N_{TS}-factor. Due to the opposite sign of PID and LID waves, a net reduction of the local wave amplitude is obtained for combined PID/LID waviness. This cancellation reflects in reduced amplitude of N-factor oscillation due to waviness.

Qualitatively, a clear correlation of wave amplitude Δz_{wave}, Δc_p, and N-factor-variation due to the wave is observed from FIG. 11 and FIG. 13. Casting this finding into a simplified ΔN-factor method for surface waviness is currently ongoing work that might lead to improved waviness allowable estimates for preliminary design in the future.

The non-negligible effect of combined PID/LID waviness on the transonic flow field is apparent from comparison of FIG. 9 (non-wavy section) and FIG. 12 (wavy section). The small surface disturbance affects the whole supersonic branch of the flow field. Nevertheless, global transonic characteristics remain intact. To emphasize on potential impact of larger wave amplitudes, results obtained with scaled waviness amplitudes are shown in FIG. 14. The formation of a multi-shock system due to increased surface disturbances is clearly visible and must be avoided. Estimated loss of laminar flow extend is -3.8%, -23.3% and -38.3% for amplitude scaling factors of 1,2 and 3, compared to the clean section without waviness.

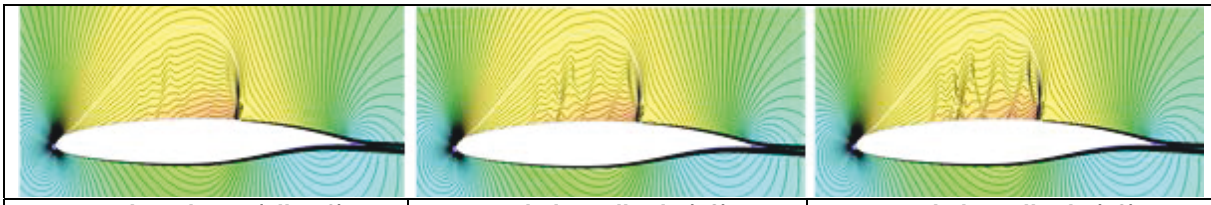

actual waviness (slice 6)	scaled amplitude (x2)	scaled amplitude (x3)

FIG. 14. Effect of scaling of surface waviness, Mach number contour & iso-lines of the flow fields

Finally, the predicted movement of transition location on the upper surface of the wing section due to spanwise varying waviness is discussed. Relative shift of transition location is shown in FIG. 15.

Upstream movement of the transition position is predicted for the waviness profiles of slices 1-6.

Despite the presence of waviness, an increase in laminar flow extend is predicted for slices no. 7-13 and 0 (reference). Here, waviness is sub-critical w.r.t. boundary layer transition but moves the shock slightly downstream, extending the laminar range. For the investigated stringer-stiffened panel, detailed analysis shows that movement of transition location is closely related to the last stringer position. With very little stability reserves of the boundary layer near mid-chord, any bump-induced deceleration will cause instantaneous transition, whereas acceleration will stabilize the flow. Although transition shift is moderate for the investigated cases (<5%), structurally induced perturbation should be avoided where the laminar boundary layer is most sensitive.

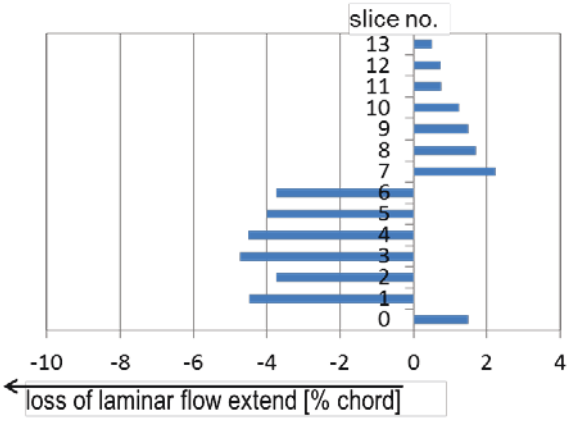

FIG. 15. Relative movement of transition location due to waviness, evaluated for 13 spanwise waviness profiles.

Because of the introduced modelling simplifications, the results presented in this study contain a non-negligible amount of uncertainty. Especially the application of local, linear stability and e^N transition prediction used for the assessment of boundary layer stability is regarded critical, since impacts of non-local, non-linear and non-parallel effects are neglected. Also the imposition of infinite swept wing flow disregards the full 3D-boundary layer and the present three-dimensionality of stringer-induced surface waviness. Nevertheless, important trends are predicted. As long as improved transition prediction methods become available for practical applications, present results are beneficial to find engineering trade-offs between aerodynamic and structural design requirements.

Note: Some scales were removed to protect intellectual rights of Airbus Group SE

Acknowledgement: The authors greatly acknowledge the fundings in the scope of LaWiPro (LuFoIV3-PTLF-74-040) and MOVE.ON-LaWOp (LuFoIV4-249-015)

8. LITERATURE

[1] Intergovernmental Panel on Climate Change, 2014: Climate Change 2014: Synthesis Report. Contribution of Working Groups I, II and III to the Fifth Assessment Report of the Intergovernmental Panel on Climate Change. IPCC, Geneva, Switzerland, 151 pp.

[2] European Commission (pub.): Flightpath 2050— Europe's vision for aviation. Publications Office of the European Union (2011)

[3] https://www.flightglobal.com/news/articles/smart-wing-design-takes-shape-for-next-generation-narrowbody-359608/ (08.04.2016)

[4] C.-C. Rossow - Aerodynamics – A discipline swept away?, The Aeronautical Journal (2010), Vol. 114 No. 1160

[5] H. Hansen - LAMINAR FLOW TECHNOLOGY – THE AIRBUS VIEW, In: ICAS 2010. Sept. 2010.

[6] A. Seitz and K.-H. Horstmann: DESIGN STUDIES ON NLF AND HLFC APPLICATIONS AT DLR, In: ICAS 2010. Sept. 2010.

[7] J. E. Green: Laminar Flow Control – Back to the Future?. 38th Fluid Dynamics Conference and Exhibit (June 2008), held by AIAA. (Seattle, Washington). http://dx.doi.org/10.2514/6.2008-3738

[8] O. Reynolds - An Experimental Investigation of the Circumstances Which Determine Whether the Motion of Water Shall Be Direct or Sinuous, and of the Law of Resistance in Parallel Channels, Phil. Trans. R. Soc. Lond. 174, 1883

[9] F. Smith, M.A. und D. J. Higton: Flight Tests on King Cobra FZ.440 to investigate the Practical Requirements for the Achievement of Low Profile Drag Coefficients on a Low Drag Aerofoil, A.R.C. RM 2375, 1945

[10] John A. Zalovcik – A Profile-drag Investigation in Flight on an Experimental Fighter-type Airplane – The North American XP-51, Technical Report, NASA-TM-79885 / NACA-ACR-245, 1942, Langley Field (VA)

[11] John A. Zalovcik et al. – Flight Investigation of Boundary-layer Transition and Profile Drag of an Experimental Low-drag Wing Installed on a Fighter-type Airplane, Wartime Report, NACA-WR-L-94 / NACA-ACR-L5C08a, 1945, Langley Field (VA)

[12] Northrop Corporation Norair Division - LFC Aircraft Design Data Laminar Flow Control Demonstration Program, Final Report No. AD0819317, 1967, Hawthorne (CA)
[13] Henry E. Payne – Laminar Flow Rethink - Using Composite Structure, Society of Automotive Engineers, Business Aircraft Meeting, Wichita (Kansas), April 6-9 1976
[14] B. J. Holmes and C. J. Obara. – Observations and implications of natural laminar flow on practical airplane surfaces, Journal of Aircraft, Vol. 20, No. 12 (1983), pp. 993-1006
[15] A. Drake and R. A. Kennelly, Jr. – Selected Experiments in Laminar Flow: An Annotated Bibliography, NASA Technical Memorandum 103989, 1992, Moffett Field, California
[16] Peter Thiede (Ed.) - Aerodynamic Drag Reduction Technologies, Proceedings of the CEAS/DragNet European Drag Reduction Conference, Potsdam, Germany, 2001
[17] Géza Schrauf - Large-Scale Laminar-Flow Tests Evaluated with Linear Stability Theory. In: Journal of Aircraft 41.2 (2004), pp. 224-230
[18] R. D. Joslin: Aircraft Laminar Flow Control. Annual Review of Fluid Mechanics 1998: vol. 30: 1-29
[19] R. D. Joslin – Overview of Laminar Flow Control, NASA/TP-1998-208705
[20] European Aviation Safety Agency – AMC-20 / Amendment 6 (2010), source: https://www.easa.europa.eu/document-library/certification-specifications/amc-20-amendment-6 (2016/09/04)
[21] Institut für Faserverbundleichtbau und Adaptronik, Braunschweig – Abschlussbericht Projekt LaWiPro (Laminar Wing Production), 2013, Technische Informationsbibliothek u. Universitätsbibliothek, Braunschweig, Hannover; 2013 https://doi.org/10.2314/GBV:78372439X
[22] Hilmar Apmann - LaWiPro - Laminar CFRP-Wing shell production : Abschlussbericht, 2013, Premium AEROTEC, Varel, Hannover; 2013, https://doi.org/10.2314/GBV:783152590
[23] Airbus Operations GmbH - Laminarflügel in CFK-Bauweise: Auslegung, Design und Validierung: LaWiPro; Abschlussbericht, Technische Informationsbibliothek u. Universitätsbibliothek, Hamburg, Hannover; 2013, https://doi.org/10.2314/GBV:790809982
[24] Deutsches Zentrum für Luft- und Raumfahrt e.V.: Verfahren zur Herstellung eines Faserverbundbauteils. Patent DE102014114012 A1. 2016/03, Deutsches Patent- und Markenamt
[25] R. F. Mann - The Probable Trend of Aeroplane Design, Article in Flight, January 3rd 1918. (https://www.flightglobal.com/pdfarchive/view/1918/1918%20-%200017.html)
[26] J. Wiedemann – Leichtbau: Elemente und Konstruktion. Springer-Verlag Berlin Heidelberg, 2007, https://doi.org/10.1007/978-3-540-33657-0
[27] A. P. Mouritz - Introduction to Aerospace Materials. Woodhead Publishing, Philadelphia, 2012
[28] Donald W. Radford - Shape Stability in Composites. Ph.D. thesis, Rensselaer Polytechnic Institute, 1987
[29] Carolyne Albert and Göran Fernlund - Spring-in and warpage of angled composite laminates, Composites Science and Technology 62 (2002), pp. 1895-1912
[30] K. D. Potter et al. - The generation of geometrical deformations due to tool/part interaction in the manufacture of composite components. Composites: Part A 36 (2005) 301-308
[31] E. Kappel - Process Distortions in Composite Manufacturing, Dissertation, 2013, Otto-von-Guericke University, Magdeburg
[32] E. Kappel et al. - Manufacturing distortions of a CFRP box-structure – A semi-numerical prediction approach (2013), Composites: Part A
[33] E. Kappel et al. - Predicting process-induced distortions in composite manufacturing – A pheno-numerical simulation strategy, Composites: Part A 51 (2013) 89–98
[34] A. Fage - The Smallest Size of a Spanwise Surface Corrugation which affects Boundary-layer Transition on an Aerofoil, RAE R&M 2120, January 1943.
[35] B. H. Carmichael - Summary of Past Experience in Natural Laminar Flow and Experimental Program for Resilient Leading Edge. NASA CR-152276 (1979)
[36] Wie, Y.S. and Malik, M.R.: Effect of surface waviness on boundary-layer transition in two-dimensional flow, Computers & Fluids 27(2):157-181,·1998, DOI: 10.1016/S0045-7930(97)00024-8
[37] Bartelheimer, W. Ein Entwurfsverfahren für Tragflügel in transsonischer Strömung. Dissertation. DLR-Forschungsbericht. 96-30, 1996
[38] N. Kroll, Description of the DLR TAU Code, Institute of Aerodynamics and Flow Technology, DLR Braunschweig, 2015, http://tau.dlr.de/code-description/
[39] Schrauf, G., LILO 2.1 User's Guide and Tutorial, Bremen, Germany, GSSC Technical Report 6, modified issue for Version 2.1, July 2006
[40] Arnal, D.: Transition Prediction based on linear theory, Progress in Transition Modelling, AGARD Report No. 793,pp 2-1 -2-63, 1994